Substituent effects on the hydrogen-bonded complex of aniline–H_2O: a computational study†

Menghui Cheng,[a] Xuemei Pu,*[ab] Ning-Bew Wong,[c] Menglong Li[a] and Anmin Tian[a]

Received (in Montpellier, France) 12th November 2007, Accepted 15th February 2008
First published as an Advance Article on the web 7th April 2008
DOI: 10.1039/b717465a

Substituent effects (X = $-CH_3$, $-NH_2$, –OH, –F, $-SiH_3$, $-PH_2$, –H, –Cl, –CN, $-NO_2$, –CHO) on the hydrogen-bonded complex of *para*-substituted aniline with one water molecule are studied at the B3LYP/6-311++G(d,p) level of theory. The nature of H-bond interactions and the origin of substituent effects are explored by means of natural bond orbital (NBO) and atoms in molecules (AIM) analysis as well as a series of good correlation equations obtained. The result suggests that the substitution induces changes in the electron density transfer from the water molecule to the aniline derivative by means of influencing the interaction of $n_O \rightarrow \sigma^*_{N-H}$ while the change in the electron density transfer would give rise to the variation on the electron densities in the proton donating N–H bond and the N–H···O hydrogen bond, and ultimately, influence the length and the frequency of the N–H bond, the H···O distance, the binding energies of complexes, the pK_a of the substituted aniline and the ^{1}H chemical shift. In addition, the correlations obtained reveals that the H-bond parameters calculated (such as $\nabla^2\rho_{H\cdots O}$, $\rho_{H\cdots O}$, $R_{H\cdots O}$), reflecting both the intramolecular (substituent effects) and intermolecular (water effects) interactions, are found to perform better than substituent constants in rationalizing the substitution induced variations on the structure, the binding energy, ^{1}H chemical shift and experimental pK_a.

1 Introduction

Studies on the intermolecular hydrogen bonding between solute and solvent molecules containing the fundamental organic functional groups using various theoretical calculations have been the subject of intense interest in recent years.[1–6] Since aniline is the simplest aromatic molecule with an amino group and a phenyl ring, the aniline–H_2O complex is a good model system to investigate the intermolecular hydrogen bond between the NH_2 group and polar solvent, which has been found to play an important role in many chemical and biological processes,[7] leading to considerable experimental and theoretical researches on it.[7–10] Spoerel and Stahl[9] investigated the rotational spectrum of aniline–water complexes by means of microwave spectrum and MP2/6-31G (d,p) method. Sakota *et al.*[10] determined the electronic and infrared spectra of jet-cooled 4-aminobenzonitrile–H_2O, followed by a theoretical study using DFT methods with cc-pVDZ basis set to provide detail structural information of the isomers. In 2006, Becucci and co-workers[11] carried out experimental and theoretical studies on the properties in the ground and excited state for the aniline–water and aniline–methanol jet cooled complexes. Recently, Szatylowicz *et al.*[12] reported dependence of the shape of NH_2 group on the substituents and H-bond formation in various aniline–small molecule (including H_2O) complexes using B3LYP and MP2 methods. Although some individual compounds or one aspect of properties of the aniline–water complex have been examined by experiments and calculations, no systematic study has been performed. It is a primary purpose of our work.

As well-known, there is considerable interest in finding correlations among molecular properties,[13–15] especially correlations of some molecular properties derived from computations and experiments with Hammett constants (σ), which have played a key part in the organization and interpretation of chemical facts and observations.[16–18] However, Hammett constants have been criticized by theoreticians because of its empirical foundation[19,20] and cannot be expected to work in all situations. For example, σ constants will fail to correlate reaction rates in situations where the change of substituent results in a shift of transition state position.[21] Furthermore, the number of available substituent constants is restricted by the necessity to carry out rigorous experimental determination. Thereby, many efforts have been devoted to investigate the applicability of other parameters as alternatives to the empirical constants. Spectroscopic data such as NMR chemical shifts, vibrational frequencies, and IR intensities have been utilized in deriving correlation equations for the evaluation of constants of new substituents[22–24] while progress of computational quantum chemistry has also offered alternative

[a] *Faculty of Chemistry, Sichuan University, Chengdu 610064, People's Republic of China*
[b] *State Key Laboratory of Biotherapy, Sichuan University, Chengdu 610064, People's Republic of China*
[c] *Department of Biology and Chemistry, City University of Hong Kong, Kowloon, Hong Kong. E-mail: xmpuscu@sina.com; Fax: +86-028-85412800*

† Electronic supplementary information (ESI) available: Fig. S1: Geometries of isolated aniline derivatives (**IA–IK**) and corresponding hydrated complexes (**IIA–IIK**) calculated at the B3LYP/-6-311++G(d,p) level of theory. Table S1: C–N Bond lengths and proton donating N–H bond lengths and stretching frequencies in all *para*-substituted aniline monomers (**I**) and the corresponding monohydrated complexes (**II**). See DOI: 10.1039/b717465a

possibilities for the situation, descriptors of which provide physical background and more accurate descriptions about electronic effects than the empirical constant. Some investigations from Chaudry and Popelier[25] and Gross *et al.*[26] revealed that some quantum chemical and quantum topological parameters are comparable with or superior to Hammett constants in describing the substituent-induced pK_a effects of anilines and phenols. Recently, Galabov, Ilieva and Schaefer[27] reported a density functional theory computational approach for the evaluation of substituent constants with the aid of theoretical electrostatic potential values.

Also, it should be noted for hydrogen-bonded systems that there is a continuing interest[28–34] in exploring correlations between some parameters describing the H-bonding, usually with an aim toward delineating and quantifying the H-bonded interaction. Some linear correlations were established between the H-bond strength (such as H-bond energies and H-bond distances) and some topological properties[28–33] (such as electron densities and Laplacian values in bond critical points) as well as electronic parameters.[34]

Based on the background and consideration above, we carried out a computational investigation of substituent effects on some properties involved in the intermolecular hydrogen bonding of the monohydrate aniline complex, such as the geometries, vibration frequencies, electronic properties, energy properties, experimental pK_a values and NMR properties. Ten para-substituted (–CH_3, –NH_2, –OH, –F, –SiH_3, –PH_2, –Cl, –CN, –NO_2, –CHO) aniline derivative–$(H_2O)_1$ complexes and the unsubstituted one are chosen for the study, where one water molecule as a proton acceptor is placed near to one hydrogen of the amino moiety as a proton donor (see Fig. 1) since the conformation of complex was determined by the electronic and infrared spectrum of 4-aminobenzonitrile–H_2O.[10] In the work, some correlations are exploited for better understanding the substituent effects. Here, we not only correlate some molecular parameters derived from calculations and experiments with the substituent σ_p constants but also derive some correlations from calculated parameters involved in the H-bonding. This study enables (1) to gain insight into the role of specific interactions (H-bonding) between the water solvent and the solute in the substituent effects (2) to probe, at least for the present system, the physical origin of substituent effects and the nature of hydrogen bonding, (3) to find other descriptors derived from quantum chemistry and quantum topological calculation and ascertain if these descriptors have caught up with or surpassed the Hammett constants in indicating variations of structure, energy and the chemical property pK_a.

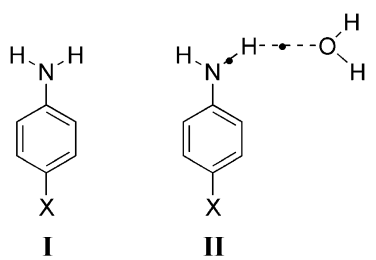

Fig. 1 Geometries of isolated aniline derivatives (**I**) and corresponding mono-hydrated complexes (**II**) calculated at the B3LYP/6-311++G(d,p) level of theory (the black dots indicate the bond critical points; X = H, CH_3, NH_2, OH, F, SiH_3, PH_2, Cl, CHO, CN, NO_2).

2 Computational details

Geometries of all the species under study are optimized by the analytic gradient technique using the density functional theory (DFT) with Becke's three parameter (B3) exchange functional along with the Lee–Yang–Parr (LYP) non-local correlation functional (B3LYP).[35] The standard Pople's 6-311++G(d,p) basis set is used in conjunction with the DFT method.[36] All stable states are verified by vibration frequency analysis at the same level of theory. Full counterpoise (CP) method is used to avoid the basis set superposition error (BSSE).[37] The corrected binding energy, ΔE_{HB}^{CP}, can be evaluated for each complex:[38] $\Delta E_{HB}^{CP} = E_{AB}^{AB}(AB) - E_{AB}^{AB}(A) - E_{AB}^{AB}(B)$ where the designations in parentheses correspond to the systems whose energies are expressed, the superscripts correspond to the basis sets used and the subscripts indicate the geometry optimized. The topological properties of electron charge densities[39] are studied by atoms in molecules (AIM) theory of Bader with AIM2000 software,[40] based on the wave function obtained at the B3LYP/6-311++G(d,p) level. Natural bond orbital (NBO) analysis introduced by Weinhold and co-workers[41] is carried out to discuss the electronic structures and orbital interactions of all the optimized structures at the same level of theory, using NBO3.1 program incorporated in Gaussian03.

The NMR chemical shifts for isolated aniline derivatives and their corresponding monohydrated complexes are calculated using "gauge-including atomic orbital" (GIAO) method[42,43] implemented into the GAUSSIAN 03 program package. The chemical shift is a difference of the chemical shielding (^{1}H) of the studied system and the chemical shielding of the reference compound tetramethylsilane, $Si(CH_3)_4$. The structure of $Si(CH_3)_4$, as a standard, is optimized at the B3LYP/6-311++G(d,p) level. To be comparable, the calculation of the nuclear shielding of the reference compound and the isolated as well as the monohydrated aniline derivative are carried out at the B3LYP/6-311++G(d,p) level of theory.

All the calculations but AIM are performed using the Gaussian03[44] series of programs. In addition, all correlation equations under study are derived using the least square fit and are verified to be significant by the *F* statistical test at the 0.01 level of significance.

3 Results and discussion

The optimized structures of substituted aniline monomers (**I**) and corresponding mono-hydrated complexes (**II**) at B3LYP/6-311++G(d,p) level are presented in Fig. S1 in ESI.† There are some studies of the geometry of aniline with experimental structures available.[3,45,46] By comparing the calculation values with the experimental one, close agreement is obtained (See Fig. S1, ESI†). The C–N bond length, the N–H bond length involved in the N–H···O contact and the corresponding vibrational stretching frequency are collected in Table 1. More detailed information concerning Table 1 can be seen in Table S1 in ESI†. Table 2 lists topological parameters of the H···O

Table 1 The C–N bond lengths (R_{C-N}/Å) and proton donating N–H bond lengths (R_{N-H}/Å) in all *para*-substituted aniline monomers (**I**) and all corresponding monohydrated complexes (**II**) and red shifts of stretching frequencies of the proton donating N–H bond ($\Delta\nu_{N-H}$/cm^{-1}) upon formation of complex calculated at the B3LYP/-6-311++G(d,p) level of theory and some corresponding experimental values (in parentheses)

	R_{C-N}		R_{N-H}		$\Delta\nu_{as\ N-H}$[a]	$\Delta\nu_{s\ N-H}$[b]
X	**I**	**II**	**I**	**II**	**II** − **I**	**II** − **I**
NH_2	1.4087	1.4030	1.0105	1.0134	−8.7	−22.1
OH	1.4059	1.4002	1.0101	1.0132	−9.1	−24.9
CH_3	1.4011	1.3946	1.0096	1.0128	−10.3	−27.7
H	1.3986	1.3915	1.0093	1.0128	−11.3 (−23.2)[cd]	−36.6 (−38.8)[cd]
F	1.4008	1.3945	1.0095	1.0129	−10.5	−30.4
PH_2	1.3931	1.3855	1.0088	1.0126	−11.2	−35.5
SiH_3	1.3928	1.3852	1.0088	1.0126	−11.6	−35.3
Cl	1.3962	1.3894	1.0090	1.0128	−11.9	−35.1
CHO	1.3816	1.3727	1.0077	1.0123	−12.7	−48.7
CN	1.3834	1.3752	1.0079	1.0125	−13.3 (−6.0)[e]	−48.8 (−25.0)[e]
NO_2	1.3776	1.3685	1.0073	1.0124	−13.8 (−33.0)[f]	−56.7 (−51.0)[f]

[a] $\Delta\nu_{as\ N-H}$ denotes the red shift of asymmetric stretching frequencies: $\Delta\nu_{as\ N-H} = \nu_{as\ N-H}$ (**II**) − $\nu_{as\ N-H}$ (**I**) [b] $\Delta\nu_{s\ N-H}$ denotes the red shift of symmetric stretching frequencies: $\Delta\nu_{s\ N-H} = \nu_{s\ N-H}$ (**II**) − $\nu_{s\ N-H}$ (**I**). [c] From ref. 48. [d] From ref. 49. [e] From ref. 10. [f] From ref. 50.

contact and the C–N bond derived from the AIM calculation, Hammett substituent constants σ_p and experiment pK_a values. Electrical parameters obtained from the NBO analysis and binding energies of the complexes are contained in Table 3 while Table 4 lists the ^{1}H chemical shift involved in the N–H···O hydrogen bond.

3.1 Geometries and vibrational analysis

It is seen on inspection of Table 1 that the N–H bond lengths involved in the N–H···O contacts lie in the range of 1.0073–1.0105 and 1.0124–1.0134 Å for the monomer and the complex, respectively. The observation shows that the substitution induced fluctuation of the N–H bond length in the monomer is slightly larger than that in the complex where the bond length appears to be insensitive to the substituents due to the effect of water molecule. As expected, the complex displays an elongation of the proton donating N–H bond by 0.0029–0.0051 Å as compared with the corresponding monomer (see Table 1 and Fig. S1, ESI†). The largest elongation (0.0051 Å) is found for the complex **IIK** with X = NO_2 while the smallest one (0.0029 Å) corresponds to the complex **IIB** with X = NH_2. Furthermore, the magnitude of N–H bond elongation (ΔR_{N-H}) displays an obvious dependence on the substituent constant, as illustrated in eqn (1) and Fig. 2(a).

$$10^3\Delta R_{N-H} = (3.5 \pm 0.1) + (1.6 \pm 0.2)\sigma_p \qquad (1)$$

$$n = 11,\ r^2 = 0.910,\ s = 0.22,\ F = 90 > F_{(1,9)} = 10.56$$

Here, n is the number of compounds, r is the correlation coefficient, s is the standard deviation, F is the F-statistics calculated and $F_{(1,9)}$ is the F critical value[47] at the 0.01 significance level. The first subscript (*i.e.*, 1) and the second one (*i.e.*, 9) of $F_{(1,9)}$ denote degrees of freedom in the numerator and denominator, respectively. As can be seen from eqn (1), the calculated F value (F = 90) is much higher than the critical F value ($F_{(1,9)}$ = 10.56), confirming the significance (or reliability) of the correlation equation. The correlation reveals that the elongation of N–H bond induced by the water molecule (ΔR_{N-H}) is enhanced by the electron-withdrawing substituent while the electron-donating substituent weakens it. At the same time, a decrease of the N–H stretching vibration is accompanied. Red shifts of 22–56 cm^{-1} are observed for the symmetric stretching vibration frequencies of the proton donating bond N–H ($\Delta\nu_{s\ N-H}$) upon complexation while the red shifts lie in the range of 8–14 cm^{-1} for the asymmetric stretching frequencies ($\Delta\nu_{as\ N-H}$), much smaller than the $\Delta\nu_{s\ N-H}$. The result calculated is consistent with some experimental observations.[10,48–50] For example, the experimental studies on the aniline[48] and aniline–$(CH_3)_2O$ cluster[49] revealed that the red shift values are 40 cm^{-1} for the N–H symmetric stretching frequency and 23 cm^{-1} for the asymmetric one (see Table 1). Also, the infrared spectrum experiment of 4-aminobenzonitrile–H_2O[10] reported that the $\Delta\nu_{s\ N-H}$ (25 cm^{-1}) is obviously larger than the $\Delta\nu_{as\ N-H}$ (6 cm^{-1}).

In agreement with the fluctuation in N–H bond elongation, the red shift of frequency would be enhanced with increase in the electron-withdrawing ability of substituents, as illustrated in eqn (2) and (3) and Fig. 2(b), where the F values calculated

Table 2 Electron densities (ρ/a.u.) and Laplacian values ($\nabla^2\rho$/a.u.) at the bond critical points for the C–N bond and the proton donating N–H bond and the H···O type H-bond derived from AIM calculation and H-bond distances ($R_{H\cdots O}$/Å) optimized at the B3LYP/6-311++G(d,p) and Hammett constants σ_P and some experimental pK_a[a]

X	ρ_{C-N}(**I**)	ρ_{C-N}(**II**)	ρ_{N-H}(**II**)	$\nabla^2\rho_{N-H}$(**II**)	$\rho_{H\cdots O}$	$\nabla^2\rho_{H\cdots O}$	$R_{H\cdots O}$	σ_P[b]	pK_a[c]
NH_2	0.2904	0.2945	0.3367	−1.6225	0.0151	0.0574	2.1503	−0.66	6.08
OH	0.2920	0.2961	0.3368	−1.6195	0.0154	0.0593	2.1366	−0.37	5.50
CH_3	0.2943	0.2989	0.3366	−1.6383	0.0156	0.0602	2.1303	−0.17	5.12
H	0.2959	0.3007	0.3365	−1.6467	0.0159	0.0614	2.1215	0.00	4.58
F	0.2951	0.2995	0.3365	−1.6430	0.0160	0.0617	2.1198	0.06	4.65
PH_2	0.2986	0.3037	0.3362	−1.6577	0.0166	0.0643	2.1026	0.05	—
SiH_3	0.2986	0.3038	0.3362	−1.6574	0.0165	0.0642	2.1034	0.10	—
Cl	0.2974	0.3021	0.3363	−1.6523	0.0165	0.0637	2.1064	0.23	3.98
CHO	0.3042	0.3100	0.3355	−1.6868	0.0178	0.0701	2.0655	0.42	—
CN	0.3038	0.3092	0.3356	−1.6817	0.0178	0.0699	2.0670	0.66	1.74
NO_2	0.3065	0.3122	0.3352	−1.6971	0.0185	0.0739	2.0483	0.78	1.02

[a] **I** Denotes the monomer and **II** denotes the complex. [b] From ref. 19. [c] From refs. 57 and 58.

Table 3 Integrated NBO analysis properties (including variations on occupation numbers (Δq/me) upon complexation for the proton donating σ^*_{N-H} orbital ($\Delta q(\sigma^*_{N-H})$) and for lone pair in the proton acceptor oxygen ($\Delta q(n_O)$) of water molecule and for the substituted aniline (Δq(ani)) and for the water molecule ($\Delta q(H_2O)$) and second-order perturbation energies ($E_{(2)}$/kcal mol^{-1}) associated with the $n_O \rightarrow \sigma^*_{N-H}$ interaction and the $n_N \rightarrow \pi^*_{C=C}$ interaction, respectively) and binding energies of complexes with inclusion of counterpoise correction for BSSE (ΔE^{CP}_{HB}/kcal mol^{-1}) calculated at the B3LYP/6-311++G(d,p) level of theory[a]

X	$\Delta q(\sigma^*_{N-H})$	$\Delta q(n_O)$	Δq(ani)	$\Delta q(H_2O)$	$E_{(2)}(n_O \rightarrow \sigma^*_{N-H})$	$E_{(2)}(n_N \rightarrow \pi^*_{C=C})$[b]	ΔE^{CP}_{HB}
NH_2	5.4	−5.7	−5.7	5.7	3.50	*22.04* (24.50)	3.20
OH	5.7	−5.9	−6.0	6.0	3.67	*23.23* (25.70)	3.46
CH_3	6.0	−6.2	−6.4	6.4	3.82	*24.73* (27.74)	3.48
H	6.4	−6.6	−6.6	6.7	4.03	*25.77* (29.98)	3.93
F	6.4	−6.6	−6.8	6.8	4.02	*25.02* (28.00)	3.64
PH_2	7.0	−7.2	−7.5	7.5	4.37	*27.73* (31.48)	4.03
SiH_3	7.0	−7.1	−7.5	7.5	4.36	*27.68* (31.53)	4.00
Cl	6.9	−7.0	−7.3	7.3	4.29	*26.51* (29.85)	4.12
CHO	8.6	−8.7	−9.3	9.3	5.22	*32.57* (38.05)	4.87
CN	8.5	−8.6	−9.0	9.0	5.17	*31.50* (36.35)	4.97
NO_2	9.4	−9.4	−10.0	10.0	5.64	— (40.29)[c]	5.37

[a] $\Delta q = q(\mathbf{II}) - q(\mathbf{I})$; **I** denotes the monomer; **II** denotes the complex; me indicates millielectron unit. [b] Monomer data in italics; complex data in parentheses. [c] — Denotes that there is no the interaction observed.

also are much larger than the critical $F_{(1,9)}$ value of 10.56 at the 0.01 significance level.

$$\Delta\nu_s = (-34.1 \pm 1.1) - (24.4 \pm 2.6)\sigma_p \quad (2)$$

$$n = 11,\ r^2 = 0.906,\ s = 3.50,\ F = 87 > F_{(1,9)} = 10.56$$

$$\Delta\nu_{as} = (-11.0 \pm 0.1) - (3.7 \pm 0.3)\sigma_p \quad (3)$$

$$n = 11,\ r^2 = 0.957,\ s = 0.352,\ F = 201 > F_{(1,9)} = 10.56$$

Since the C–N bond connecting the amino group with the phenyl group is an appropriate monitor of the degree of delocalization between the two fragments,[25] it is important to discuss the C–N bond length variation both in the monomer and the complex. As shown in eqn (4) and (5), the C–N bond lengths, either in the monomers (R_{C-N} (**I**)) or in the complexes (R_{C-N} (**II**)), obviously correlate with the substituent constant.

Table 4 GIAO B3LYP/6-311++G(d,p) calculated ^{1}H chemical shifts (δ_H/ppm) of the amino group hydrogen nucleus involved in the H-bonding for the monomer (**I**) and the complex (**II**) and variations of ^{1}H chemical shifts upon complexation ($\Delta\delta_H$/ppm) and some corresponding experimental values (δ_H/ppm)

	δ_H		$\Delta\delta_H$	Experimental δ_H	
X	**I**	**II**	**II** − **I**	$CDCl_3$[a]	DMSO-d_s[b]
NH_2	2.82	5.05	2.23	3.30	—
OH	2.91	5.18	2.27	—	4.36[a]
CH_3	3.08	5.39	2.31	3.49	4.70
H	3.21	5.56	2.35	3.55	4.90
F	3.09	5.45	2.36	3.45	4.88
PH_2	3.30	5.77	2.47	—	—
SiH_3	3.30	5.76	2.46	—	—
Cl	3.16	5.60	2.44	3.57	5.15
CHO	3.64	6.32	2.68	—	—
CN	3.56	6.19	2.63	4.30	—
NO_2	3.78	6.53	2.75	—	6.63

[a] Chemical shifts were referred to TMS in deuteriochloroform solutions.[61] [b] Chemical shifts were referred to TMS in deuterated dimethyl sulfoxide solutions.[62]

$$R_{C-N}(\mathbf{I}) = (1.3968 \pm 0.0011) - (0.023 \pm 0.003)\sigma_p \quad (4)$$

$$n = 11,\ r^2 = 0.894,\ s = 0.0035,\ F = 76 > F_{(1,9)} = 10.56$$

$$R_{C-N}(\mathbf{II}) = (1.3898 \pm 0.0012) - (0.025 \pm 0.003)\sigma_p \quad (5)$$

$$n = 11,\ r^2 = 0.886,\ s = 0.0040,\ F = 70 > F_{(1,9)} = 10.56$$

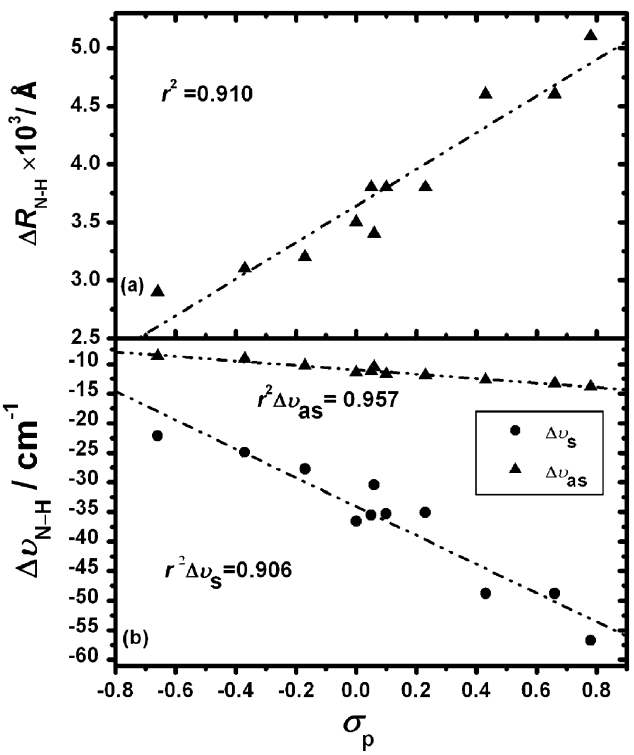

Fig. 2 Dependences of the elongation of N–H bond length (10^3 ΔR_{N-H}/Å) and the red shift of N–H stretching frequency (including symmetric stretching frequency ($\Delta\nu_s$/cm^{-1}) and asymmetric stretching frequency ($\Delta\nu_{as}$/cm^{-1})) on the Hammett constant (σ_p).

The correlation coefficients (r^2) and the coefficients before the σ_p in eqns (4) and (5) imply that the linear dependence is almost retained with the transition from the isolated monomer to the complex and the C–N bond length display a reverse dependence on the electron-donating ability of substituents both in the monomer and the complex. Interestingly, the C–N bond length is shortened by 0.0057–0.0091 Å (see Table 1) upon formation of complex, implying that the water solvent may enhance the electron density delocalization between the amino group and the phenyl ring. More detail analysis of the variation on the C–N bond will be done below on the basis of the AIM and NBO computations.

3.2 AIM and NBO analysis

To gain more insight into the H-bond characteristics, the electron density topological analysis based on the AIM theory is carried out for all the monomers and the complexes considered here. The rigorous AIM theory has been successfully applied in characterizing hydrogen bonds of different strengths in a wide variety of molecular complexes.[33] Recently, Koch and Popelier mentioned some topological criteria based on the AIM theory[51,52] to detect and characterize the hydrogen bonding. The most prominent evidence of hydrogen bonding is: (i) correct topological pattern (*i.e.*, the existence of a bond critical point (BCP) and a bond path); (ii) proper value of electron density and Laplacian of electron density at this BCP. These topologic properties calculated using the AIM2000 program are listed in Table 2 and illustrated in Fig. S1, ESI.†

In terms of the AIM calculation results, a bond critical point (BCP) in the H···O contact is found for all the complexes and the bond path of the BCP links the oxygen atom of water molecule and one hydrogen of the amino group of aniline derivative, as visualized in Fig. 1 and Fig. S1, ESI.† The corresponding Laplacian values of electron densities at the BCPs ($\nabla^2\rho_{H\cdots O}$) lie within 0.0574–0.0740 a.u. and the electron densities at the BCPs ($\rho_{H\cdots O}$) in all complexes range between 0.0151 and 0.0186 a.u., much smaller than that of a covalent bond. These results clearly indicate that the H···O contacts are classical hydrogen bonding ($\rho \approx 10^{-2}$ and positive $\nabla^2\rho$).[32] A comparison of the substituted complex with the unsubstituted one shows that the electron-withdrawing substituent increase the $\rho_{H\cdots O}$ and $\nabla^2\rho_{H\cdots O}$ and shorten the $R_{H\cdots O}$ while the electron-donating one has an opposite effect, as seen in Table 2.

To further understand the nature of hydrogen bonding interaction, the NBO analysis is carried out at the B3LYP/6-311++G(d,p) level of theory. All related data derived from the NBO calculation are summarized in Table 3. The data in Table 3 shows that the intermolecular electron density transfers (Δq(ani), $\Delta q(H_2O)$) from the water molecule to the substituted aniline are in the range of 5.7–10.0 me upon complexation. In addition, the NBO analysis reveals that lone pair of oxygen atom of the water molecule (n_O) interacts with σ antibonding orbital of the N–H bond of aniline derivative (σ^*_{N-H}) for all the complexes and interaction energies $E_{(2)}$ associated with the $n_O \rightarrow \sigma^*_{N-H}$ range from 3.50 to 5.64 kcal mol^{-1}. The $n_O \rightarrow \sigma^*_{N-H}$ delocalization leads to a decrease of 5.7–9.4 me in electron density at the n_O of the water molecule and an almost equal electron density increment of 5.4–9.4 me in the σ^*_{N-H} ($\Delta q(\sigma^*_{N-H})$) involved in the N–H···O contact (see Table 3), which is also nearly equal to the total amount of intermolecular charge transfer (5.7–10.0 me). The observation clearly show that the electron density transfer from the water molecule to the substituted aniline mainly stem from the electron delocalization from the n_O of the water to the σ^*_{N-H} of the aniline derivative. An excellent linear relationship (see Fig. 3(a)) is obtained with $r^2 = 0.999$ between the $E_{(2)}(n_O \rightarrow \sigma^*_{N-H})$ and the $\Delta q(\sigma^*_{N-H})$, further confirming that it is the $n_O \rightarrow \sigma^*_{N-H}$ delocalization that results in an increase of electron density in the σ^*_{N-H} orbital. Another excellent linear relationship with $r^2 = 0.995$ (see Fig. 3(b)) is found between the $\Delta q(\sigma^*_{N-H})$ and the ΔR_{N-H}, clearly indicating that the elongation of the N–H bond (ΔR_{N-H}) is attributed to the increase of electron density in the σ^*_{N-H} orbital upon complexation, consistent with the behavior of red-shifted H-bonds.[6]

In addition, a satisfactory linear relationship presented by eqn (6) shows the substituent effect on the $n_O \rightarrow \sigma^*_{N-H}$ interaction that the electron-withdrawing group enhances the $n_O \rightarrow \sigma^*_{N-H}$ interaction while the electron-donating one diminishes it.

$$E_{(2)} = (4.22 \pm 0.007) + (1.55 \pm 0.17)\sigma_p \qquad (6)$$

$$n = 11,\ r^2 = 0.899,\ s = 0.231,\ F = 80 > F_{(1,9)} = 10.56$$

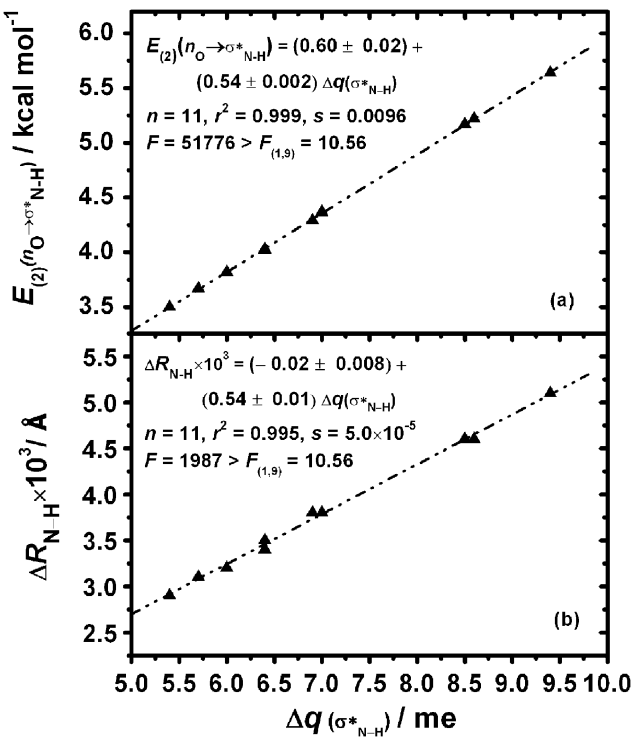

Fig. 3 The correlations of the electron density increase in the σ^*_{N-H} orbital of complexes ($\Delta q(\sigma^*_{N-H})$/me) with the interaction energy ($E_{(2)}(n_O \rightarrow \sigma^*_{N-H})$/kcal mol^{-1}) and the elongation of N–H bond (ΔR_{N-H}/Å) involving the N–H···O contact.

By means of the correlations derived from eqn (6) and Fig. 3, we can explain the origin of substituent effect on the N–H bond elongation, *viz*. the origin of the eqn (1) presented in the geometric discussions above. The substituent first influence the $n_O \rightarrow \sigma^*_{N-H}$ interaction ($E_{(2)}$) and then leads to the variation on the electron density increment of the σ^*_{N-H} orbital ($\Delta q(\sigma^*_{N-H})$), and ultimately influence the magnitude of N–H bond elongation (ΔR_{N-H}). In terms of the origin observed, the magnitude of N–H bond elongation is a direct consequence of electron density variation in the σ^*_{N-H} orbital induced by the water molecule and the substituent group. Therefore, the correlation coefficient associating with the $\Delta q(\sigma^*_{N-H})$ and the ΔR_{N-H} is obviously higher than that between the ΔR_{N-H} and the substituent constant σ_p ($r^2 = 0.910$, see eqn (1) and Fig. 2a), suggesting that the $\Delta q(\sigma^*_{N-H})$ may act as a better indicator than the substituent constant in describing the variation on the elongation of the N–H bond.

As suggested in the geometry discussion concerning the C–N bond length above, the water molecule may enhance the charge density delocalization from the amino group to the phenyl π-system. In fact, the NBO calculation shows that the interaction energy $E_{(2)}$ associated with the $n_N \rightarrow \pi^*_{C=C}$ delocalization is greater in the complex than that in the monomer, as can be found in Table 3. It is reasonable for the complex system to assume that the increment in the $E_{(2)}(n_N \rightarrow \pi^*_{C=C})$ should lead to a rise of the charge density in the C–N bond critical point (ρ_{C-N}). As expected, the ρ_{C-N} value of complex is larger than that of monomer (Table 2) and a good linear correlation with $r^2 = 0.987$ (see Fig. 4(a)) is established

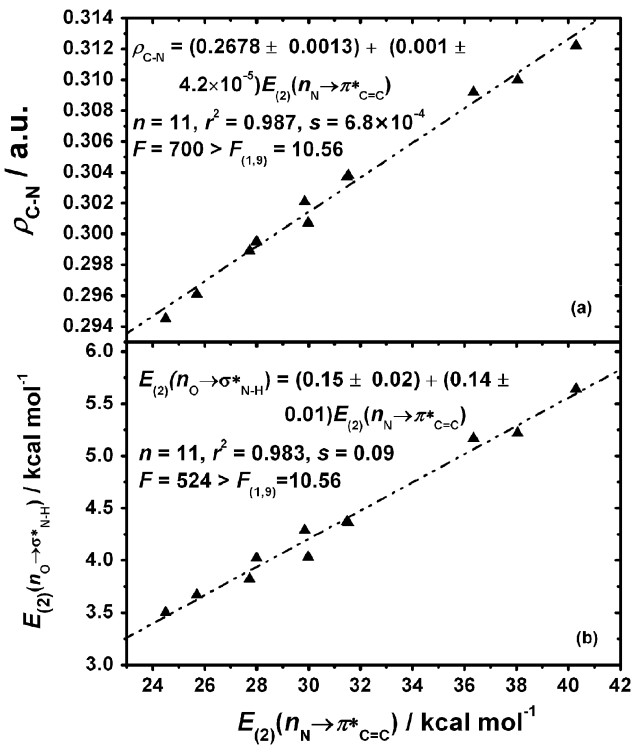

Fig. 4 The correlations of the delocalization effect examined by the ($E_{(2)}(n_N \rightarrow \pi^*_{C=C})$/kcal mol^{-1}) with the H-bonding interaction characterized by ($E_{(2)}(n_O \rightarrow \sigma^*_{N-H})$/kcal mol^{-1}) and the electron density at the BCP of C–N bond (ρ_{C-N}/a.u.).

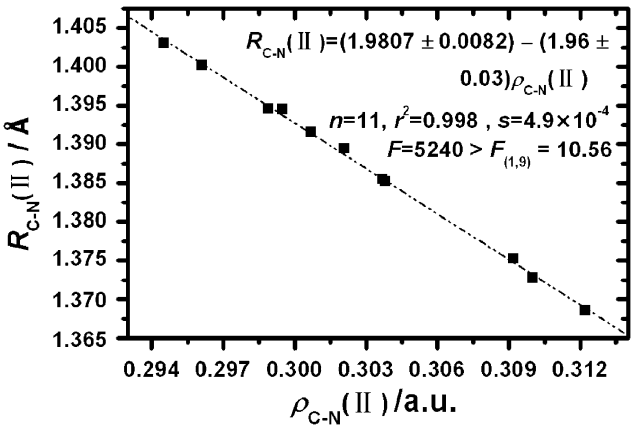

Fig. 5 The correlation of the electron density at the BCP of C–N bond (ρ_{C-N}(**II**)) with the C–N bond length (R_{C-N}(**II**)) for all the complexes.

between the $E_{(2)}(n_N \rightarrow \pi^*_{C=C})$ values and the ρ_{C-N} values, providing a support for the assumption. The increase in ρ_{C-N} upon complexation leads to a decrease in the C–N bond length (R_{C-N}), evidenced by an almost perfect linear correlation ($r^2 = 0.998$) between the R_{C-N} and the ρ_{C-N} (Fig. 5). In addition, another good correlation with $r^2 = 0.983$ between the $E_{(2)}(n_N \rightarrow \pi^*_{C=C})$ and the $E_{(2)}(n_O \rightarrow \sigma^*_{N-H})$ (see Fig. 4(b)) further reveal that the enhanced $n_N \rightarrow \pi^*_{C=C}$ delocalization upon formation of complex is attributed to the specific H-bond interaction derived from the water solvent.

3.3 Energy analysis

Binding energies of complexes, when accurately computed, can yield direct estimation of the solvent–solute interactions measured in molecular scale. Thereby, we calculate the binding energies (ΔE^{CP}_{HB}) of the eleven substituted aniline–H_2O complexes using the full counterpoise optimization to avoid the BSSE, and analyze variations on the binding energies caused by the substituents. In agreement with the above geometric results, the largest binding energy also comes from the NO_2 substitution (5.37 kcal mol^{-1}) and the smallest binding energy corresponds to the NH_2 substitution (3.20 kcal mol^{-1}). A satisfactory correlation is obtained between the binding energy (ΔE^{CP}_{HB}) and the substituent constant with $r^2 = 0.909$, as shown in eqn (7).

$$\Delta E^{CP}_{HB} = (3.94 \pm 0.07) + (1.57 \pm 0.17)\sigma_p \qquad (7)$$

$$n = 11,\ r^2 = 0.909,\ s = 0.221,\ F = 90 > F_{(1,9)} = 10.56$$

The equation reveals that the binding energy becomes larger as the substituent becomes more electron-abstracting. Better linear relationships, however, are found between the ΔE^{CP}_{HB} and some H-bond parameters such as $\nabla^2\rho_{H\cdots O}$, $\rho_{H\cdots O}$ and $R_{H\cdots O}$, as shown in Fig. 6. The correlation coefficients (r^2) relating these quantities and the binding energies are 0.977 for the H···O distance ($R_{H\cdots O}$), 0.979 for the Laplacian of the electron density at the BCP ($\nabla^2\rho_{H\cdots O}$) and 0.980 for the electron density at the BCP ($\rho_{H\cdots O}$), much higher than that associated with the substituent constant ($r^2 = 0.909$). The

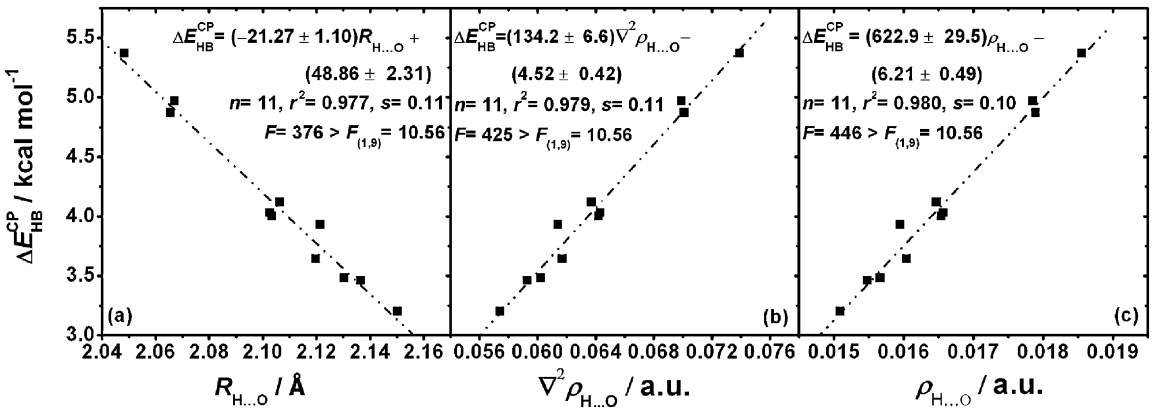

Fig. 6 Dependences of the binding energy of complexes (ΔE_{HB}^{CP}/kcal mol^{-1}) on (a) the H···O distance ($R_{H\cdots O}$/Å); (b) the Laplacian value of the H···O contact ($\nabla^2\rho_{H\cdots O}$/a.u.); (c) the electronic density in the H···O contact ($\rho_{H\cdots O}$/a.u.).

observations suggest that the H-bond parameters can act as better descriptors than the substituent constant in indicating the variation of binding energies. At the same time, the three H-bond parameters ($\nabla^2\rho_{H\cdots O}$, $\rho_{H\cdots O}$, $R_{H\cdots O}$) display strongly linear dependences on the interaction energy $E_{(2)}(n_O \rightarrow \sigma^*_{N-H})$, as depicted in eqn (8)–(10). Whereas, the $E_{(2)}(n_O \rightarrow \sigma^*_{N-H})$ was already found to obviously correlate with the substituent constant (see eqn (6) above).

$$\rho_{H\cdots O} = (0.0096 \pm 0.0001) + (0.0016 \pm 0.0000)E_{(2)} \quad (8)$$

$$n = 11,\ r^2 = 0.997,\ s = 6.25 \times 10^{-5},\ F = 3053 > F_{(1,9)} = 10.56$$

$$\nabla^2\rho_{H\cdots O} = (0.0318 \pm 0.0005) + (0.0074 \pm 0.0001)E_{(2)} \quad (9)$$

$$n = 11,\ r^2 = 0.999,\ s = 2.61\times10^{-4},\ F = 3837 > F_{(1,9)} = 10.56$$

$$R_{H\cdots O} = (2.3085 \pm 0.0047) - (0.0466 \pm 0.0011)E_{(2)} \quad (10)$$

$$n = 11,\ r^2 = 0.995,\ s = 0.007,\ F = 1938 > F_{(1,9)} = 10.56$$

In terms of the series of correlations suggested by Fig. 6 and eqn (8) and (9) as well as eqn (6), we also explain the origin of the substituent effect on the binding energy (ΔE_{HB}^{CP}), *viz*. the origin of correlation expressed by eqn (7). The electron-withdrawing substituent enhance the $n_O \rightarrow \sigma^*_{N-H}$ interaction (see eqn (6)) and induces more electron density transfers from the water molecule to the aniline derivative, and accordingly increases the $\rho_{H\cdots O}$ and shortens the $R_{H\cdots O}$ (see eqn (8)–(10)). Ultimately, the interaction of the water molecule and the solute molecule is enhanced (see Fig. 6), as reflected by larger ΔE_{HB}^{CP}. Conversely, the electron-donating substituent disfavor the $n_O \rightarrow \sigma^*_{N-H}$ interaction, and leads to lower $\rho_{H\cdots O}$ value, longer $R_{H\cdots O}$ and smaller ΔE_{HB}^{CP}. Similarly, the origin suggests that the fluctuations in the binding energy caused by the substitution is a direct consequence of the variations of the H···O bond (*i.e*., electron density and bond length) while the substituent induces the changes in the H···O bond through influencing the $n_O \rightarrow \sigma^*_{N-H}$ interaction (*viz*., the H-bonding interaction between the water molecule and the substituted aniline). Thereby, the three H-bonding parameters ($\nabla^2\rho_{H\cdots O}$, $\rho_{H\cdots O}$ and $R_{H\cdots O}$), which reflect both the intramolecular (substituent effects) and intermolecular (water effects) interactions, perform better than the substituent constant in describing the substituent-induced energy effects, as reflected by higher correlation coefficients in Fig. 6 above.

3.4 Dependence of pK_a upon H-bond interaction and estimation of pK_a

Since the amino moiety is one of the most fundamental organic functional groups, its pK_a is an important and extensively studied property. The pK_a here refers to the conjugate acids, but it is used as a measure of the amine's basicity since pK_a + pK_b = pK_w, where K_w is the ionization constant of water. Variations in pK_a are crucial to the action of enzymes,[53] RNA activity in protein synthesis[54] and pharmokinetic properties[55] in pharmaceutical industry. Thus, the ability to predict the pK_a quantitatively in a wide variety of chemical systems is still actively pursued in some research groups. Chaudry and Popelier[25] and Seybold and co-workers[26] employed some quantum chemical parameters and quantum topological descriptors derived from computational results of isolated molecules, without considering the solvent effect, to obtain correlation equations for evaluation of the experimental pK_a values of substituted anilines. As known from both experiments and theories, solvents may induce considerable changes in the chemical reaction[27] while the H-bond may be treated as an acid–base interaction in terms of the Brønsted–Lowry formalism.[33,56] Therefore, it may be more reasonable to take into account the specific H-bond interaction between the solute and solvent when estimating on the variation in pK_a induced by substitutions. Similarly, we explore correlations between the pK_a value with the three H-bonding parameters ($\nabla^2\rho_{H\cdots O}$, $\rho_{H\cdots O}$ and $R_{H\cdots O}$). Of eleven substituted aniline studied here, only the pK_a values of eight aniline derivatives are available from experiments[57,58] (excepting for the PH_2, SiH_3, and CHO groups, see Table 2). As expected, excellent linear relationships are obtained between the pK_a of the eight aniline derivatives and the three H-bond parameters

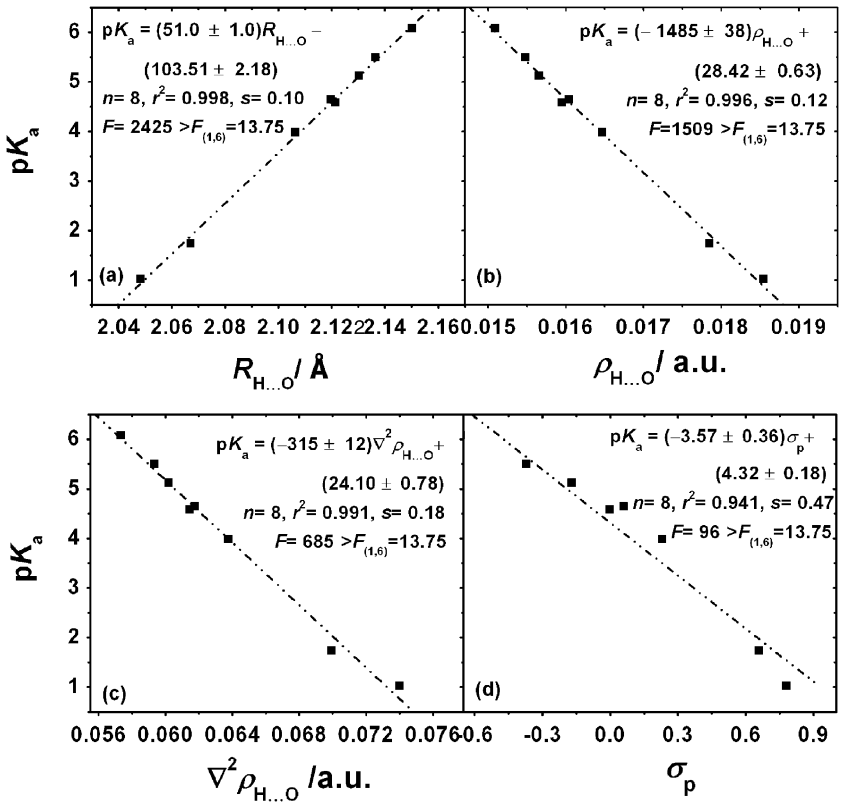

Fig. 7 Dependences of the experimental pK_a value of the eight substituted anilines apart from the three derivatives respectively substituted by the CHO, PH_2 and SiH_3 groups on (a) the H···O distance ($R_{H\cdots O}$/Å); (b) the electronic density in the H···O contact ($\rho_{H\cdots O}$/a.u.); (c) the Laplacian value in the H···O contact ($\nabla^2\rho_{H\cdots O}$/a.u.); (d) Hammett constants (σ_p).

with r^2 = 0.991–0.998 (see Fig. 7(a)–(c)), obviously higher than that associated the pK_a against the Hammett substituent constants (r^2 = 0.941), as shown in Fig. 7(d). The result confirms that the including of specific solvent effect would lead to better results and the H-bond parameters are more effective than the Hammett constants in describing the substitution induced pK_a variation.

These calculated F values in Fig. 7(a)–(d) are much higher than the $F_{(1,6)}$ critical value of 13.75 at the 0.01 significance level, demonstrating the significance of these correlations. By means of the correlation equations in Fig. 7(a)–(c), some pK_a values may be predicted for aniline derivatives without experimental values available, like the aniline derivatives substituted by the PH_2, SiH_3 and CHO groups in the study. The average values of pK_a estimated by Fig. 7(a)–(c) are about 3.78 for the PH_2 substitution, 3.84 for the SiH_3 substitution and 1.95 for the CHO substitution.

3.5 NMR data analysis

As well-known, infrared spectroscopy has been the most often applied spectroscopic tool to determine the existence of hydrogen bonding. There are, however, a number of NMR observables that also provide indirect evidence for the formation of a hydrogen bond, perhaps the most characteristic being a large downfield chemical shift of the hydrogen-bonded proton relative to the monomer since the exposure of the delocalized proton decreases the electron density around the H nucleus, shifting the NMR signal to higher frequency (low field).[59,60] Hence, the NMR chemical shieldings of isolated aniline derivatives and their corresponding monohydrated complexes are calculated using gauge-including atomic orbital (GIAO) method at the B3LYP/6-311++G(d,p) level of theory. The calculated ^{1}H chemical shifts of amino group hydrogen atom involved in the N–H···O contact are listed in Table 4, along with experimental values available for some para-substituted aniline derivatives in deuterated chloroform ($CDCl_3$) and dimethyl sulfoxide (DMSO-d_6) solutions.[61,62]

Inspection of the experimental data in Table 4 shows that the ^{1}H chemical shifts (δ_H) are dependent on the solvent employed, as reported in many researches.[63–65] The δ_H value in the DMSO-d_6 is obviously larger than that in the $CDCl_3$ solution since the dimethyl sulfoxide is more polar and better hydrogen bonding solvent.[63] By comparison, a good agreement can be found between the experimental δ_H value from the $CDCl_3$ solution and the calculated δ_H value in the monomer while the experimental δ_H value from the DMSO-d_6 solution is close to the calculated δ_H value in the complex. An excellent linear correlation with r^2 = 0.993 is obtained between the experimental δ_H value from DMSO-d_6 solution and the calculated one in the complex, as shown in Fig. 8. These findings imply that there should be a hydrogen bonding interaction between the amino group of aniline derivatives and the DMSO solvent in the experimental determination while

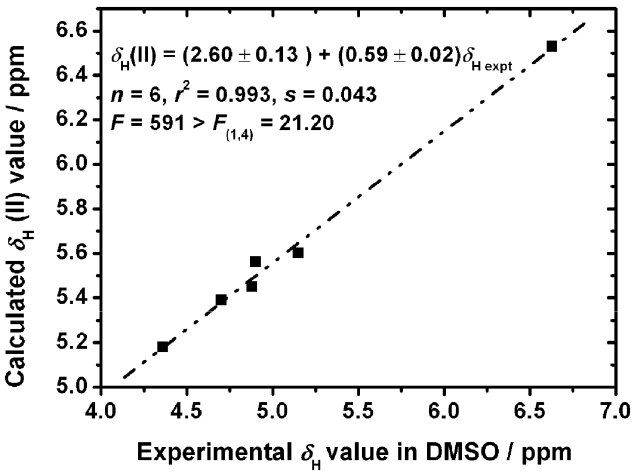

Fig. 8 The correlation of calculated ^{1}H chemical shifts (δ_H/ppm) with the corresponding experimental values in DMSO-d_6 solution.

the H-bonding interaction between the solute and the solvent may be not existed in the experimental determination employing the $CDCl_3$ as solvent since the experimental δ_H value from the $CDCl_3$ solution is close to that of monomer calculated. In addition, the correlation presented by Fig. 8 may provide an additional support for the observations[63] that the solvent effect on the labile proton chemical shifts can be attributed to the dominant interaction of hydrogen bonding.

As can be seen from the calculated δ_H values in Table 4, strongly electron-withdrawing groups (such as NO_2, CN and CHO) lead to an increase of the ^{1}H chemical shift compared with the unsubstituted aniline whereas electron-donating substituents (for example, NH_2, OH, CH_3) result in a decrease, either in the complex or in the monomer, in accordance with the experimental results listed in Table 4.

It is seen on inspection of Table 4 that the nuclear shifts of amino group hydrogen atom involved in the H-bonding in the complex is 2–3 ppm higher than those in the corresponding isolated aniline derivative. The variation in the ^{1}H chemical shift ($\Delta\delta_H$) upon formation of complex displays excellent linear dependences on the electron density $\rho_{H\cdots O}$, the Laplacian value $\nabla^2\rho_{H\cdots O}$ and the hydrogen bond distance $R_{H\cdots O}$, as illustrated in Fig. 9. Exponential relationships between proton chemical shifts and AIM topological descriptors were founded in the short strong hydrogen bond system[66] while similar linear correlations were reported in some intramolecular hydrogen bond system.[60] On the other side, the $\Delta\delta_H$ values correlate well the binding energies (ΔE_{HB}^{CP}), as shown in eqn (11).

$$\Delta E_{HB}^{CP} = (-5.64 \pm 0.62) + (3.98 \pm 0.25)\Delta\delta_H \qquad (11)$$

$$n = 11,\ r^2 = 0.965,\ s = 0.14,\ F = 248 > F_{(1,9)} = 10.56$$

The linear relationships presented by Fig. 9 and eqn (11) further demonstrate the connection of NMR spectroscopic properties and the H-boning interaction and may help to establish the H-bond features associated with NMR shifts. Especially, the excellent correlation between the $\Delta\delta_H$ and the electron density $\rho_{H\cdots O}$ provides a clear evidence for the fact that the strong deshielding is a direct consequence of electron redistribution around the H atom occurring upon hydrogen bonding.

$$\Delta\delta_H = (2.41 \pm 0.02) - (0.38 \pm 0.05)\sigma_p \qquad (12)$$

$$n = 11,\ r^2 = 0.867,\ s = 0.063,\ F = 66 > F_{(1,9)} = 10.56$$

On the other hand, the $\Delta\delta_H$ displays a dependence on the substituents, as presented in eqn (12), suggesting that the $\Delta\delta_H$ would be enhanced with increase in the electron-withdrawing ability of substituents. Similarly, the substituent effect can be rationalized by the series of correlations presented by eqn (6), (8) and (9), and Fig. 9. The electron-withdrawing group favors the $n_O \rightarrow \sigma^*_{N-H}$ interaction and leads to higher $\rho_{H\cdots O}$ value and lower electron density around the H nucleus as compared with the electron-donating substituent. Also, the correlation coefficient associated with the substituent constant (r^2 = 0.867) is significantly lower that those associated with the H-bonding parameters (r^2 = 0.991–0.993, see Fig. 9).

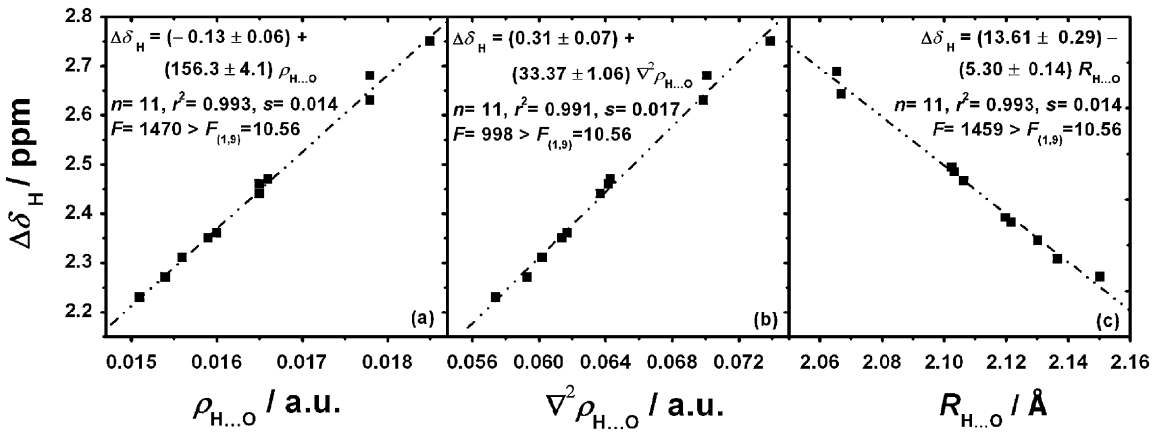

Fig. 9 Dependences of the calculated ^{1}H chemical shift variation ($\Delta\delta_H$/ppm) induced by the H-bonding on (a) the electronic density in the H···O contact ($\rho_{H\cdots O}$/a.u.); (b) the Laplacian value in the H···O contact ($\nabla^2\rho_{H\cdots O}$/a.u.); (c) the H···O distance ($R_{H\cdots O}$/Å).

4 Conclusions

In this work, the eleven monomers of aniline derivatives and their monohydrated complexes are optimized at the level of B3LYP/6-311++G(d,p) theory. The correlation analysis, together with NBO and AIM methods, are applied to investigate the nature of H-bond interaction and the physical origin of substituent effects. Some satisfactory and excellent linear relationships are established. In terms of these correlations, the effect of substituents on the H-bond interaction of complexes are attributed to the substitution induced variation of the electron density transfer from the water molecule to the aniline derivative by means of influencing the interaction of $n_O \rightarrow \sigma^*_{N-H}$ while the change in the electron density transfer would give rise to the variation on the electron densities in the N–H bond and H···O contact, and ultimately, influence the length and the frequency of the proton donating N–H bond, the H···O distance, the binding energies of complexes, the pK_a of the substituted aniline and the ^{1}H chemical shift. In addition, the correlations obtained reveal that the charge density delocalization from the amino group to the phenyl group is enhanced by the water molecule through the H-bond interaction, which leads to the decrease of C–N bond length upon the formation of complex. Our results show that it is important to consider the specific intermolecular interaction between the solute and the solvent when investigating some properties in solution. Thereby, the H-bond parameters (such as $\nabla^2\rho_{H\cdots O}$, $\rho_{H\cdots O}$, $R_{H\cdots O}$), reflecting both the intramolecular (substituent effects) and intermolecular (water effects) interactions, are found to perform better than the substituent constant in rationalizing the substitution induced variations on the binding energy of complex, the ^{1}H chemical shift and the pK_a of the aniline derivatives, and may be applied to estimate pK_a values of aniline derivatives that are unable to analysis *via* Hammett parameters such as when values are not obtainable for the fragments under observation. The result confirms the reliability of descriptors derived from quantum chemistry and quantum topological computation and suggests that the computational approach may provide an alternative possibility for estimating some molecular properties without performing rigorous experiments.

Acknowledgements

This project is supported by the National Science Foundation of China (Grant No 20775052) and N.-B. W. acknowledges the support of a Strategic Grant from City University of Hong Kong (Account No. 7001974). Helpful suggestions from Prof. Y. Ren and Prof. H. W. Zhou are also deeply acknowledged.

References

1 G. A. Kumar and M. A. McAllister, *J. Am. Chem. Soc.*, 1998, **120**, 3159–3165.
2 D.-S. Ahn, S. Park, S.-W. Lee and B. Kim, *J. Phys. Chem. A*, 2003, **107**, 131–139.
3 M. E. Vaschetto, B. A. Retamal and A. P. Monkman, *J. Mol. Struct. (THEOCHEM)*, 1999, **468**, 209–221.
4 W. D. He, Y. Xue, H. Zhang and A. M. Tian, *J. Phys. Chem. B*, 2006, **110**, 1416–1422.
5 G. C. Pimental and A. L. McClellan, *The Hydrogen Bond*, Freeman, San Francisco, CA, 1960.
6 E. Mrázková and P. Hobza, *J. Phys. Chem. A*, 2003, **107**, 1032–1039.
7 L. Yang, J. S. Dordick and S. Garde, *Biophys. J.*, 2004, **87**, 812–821.
8 A. K. Chandra, M. T. Nguyen, T. Uchimaru and Th. Zeegers-Huyskens, *J. Mol. Struct. (THEOCHEM)*, 2000, **555**, 61–66.
9 U. Spoerel and W. Stahl, *J. Mol. Spectrosc.*, 1998, **190**, 278–289.
10 K. Sakota, N. Yamamoto, K. Ohashi, H. Sekiya, M. Saeki, S.-I. Ishiuchi, M. Sakai and M. Fujii, *Chem. Phys. Lett.*, 2001, **341**, 70–76.
11 G. Piani, M. Pasquini, I. López-Tocón, G. Pietraperzia, M. Becucci and E. Castellucci, *Chem. Phys.*, 2006, **330**, 138–145.
12 H. Szatylowicz, T. Krygowski and M. P. Hobza, *J. Phys. Chem. A*, 2007, **111**, 170–175.
13 D. Colon, E. J. Weber and G. L. Baughman, *Environ. Sci. Technol.*, 2002, **36**, 2443–2450.
14 S. J. Grabowski, *J. Phys. Chem. A*, 2000, **104**, 5551–5557.
15 L. Liu, Q.-X. Guo and Y. Feng, *J. Phys. Chem. A*, 2002, **106**, 11518–11525.
16 X. M. Pu, N.-B. Wong, G. Zhou and A. M. Tian, *Chem. Phys. Lett.*, 2005, **408**, 101–106.
17 B. Galabov, S. Ilieva, B. Hadjieva and E. Dinchova, *J. Phys. Chem. A*, 2003, **107**, 5854–5861.
18 P.-C. Nam, M. T. Nguyen and A. K. Chandra, *J. Phys. Chem. A*, 2006, **110**, 4509–4515.
19 C. Hansch, A. Leo and R. W. Taft, *Chem. Rev.*, 1991, **91**, 165–195.
20 L. T. Kanervat and A. M. Klibanov, *J. Am. Chem. Soc.*, 1989, **111**, 6865–6866.
21 T. H. Lowry and K. S. Richardson, *Mechanism and Theory in Organic Chemistry*, Harper Collins, New York, 3rd edn, 1987.
22 D. J. Craik and R. T. C. Brownlee, *Prog. Phys. Org. Chem.*, 1983, **14**, 1–73.
23 A. R. Katritzky and R. D. Topsom, *Chem. Rev.*, 1977, **77**, 639–658.
24 (*a*) R. D. Topsom, *Prog. Phys. Org. Chem.*, 1987, **14**, 193–235; (*b*) E. A. Velcheva, I. N. Juchnovski and I. G. Binev, *Spectrochim. Acta, Part A*, 2003, **59**, 1745–1749.
25 U. A. Chaudry and P. L. A. Popelier, *J. Org. Chem.*, 2004, **69**, 233–241.
26 K. C. Gross, P. G. Seybold, Z. Peralta-Inga, J.S. Murray and P. Politzer, *J. Org. Chem.*, 2001, **66**, 6919–6925.
27 B. Galabov, S. Ilieva and H. F. Schaefer, *J. Org. Chem.*, 2006, **71**, 6382–6387.
28 D.-L. Wu, L. Liu, G.-F. Liu and D.-Z. Jia, *J. Phys. Chem. A*, 2007, **111**, 5244–5252.
29 R. Parthasarathi, S. Sundar Raman, V. Subramanian and T. Ramasami, *J. Phys. Chem. A*, 2007, **111**, 7141–7148.
30 L. Senthilkumar, T. K. Ghanty and S. K. Ghosh, *J. Phys. Chem. A*, 2005, **109**, 7575–7582.
31 I. Alkorta and J. Elguero, *J. Am. Chem. Soc.*, 2002, **124**, 1488–1493.
32 I. Rozas, I. Alkorta and J. Elguero, *J. Phys. Chem. B*, 2004, **108**, 3335–3341.
33 S. J. Grabowski, *Annu. Rep. Prog. Chem., Sect. C*, 2006, **102**, 131–165.
34 G. Oliveira, F. S. Pereira, R. C. M. U. de Araújo and M. N. Ramos, *Chem. Phys. Lett.*, 2006, **427**, 181–184.
35 (*a*) C. Lee, W. Yang and R. G. Parr, *Phys. Rev. B*, 1988, **37**, 785–789; (*b*) W. Kohn and A. D. Becke, *J. Phys. Chem.*, 1996, **100**, 12974–12980; (*c*) P. J. Stephens, F. J. Devlin, C. F. Chabalowski and M. J. Frisch, *J. Phys. Chem.*, 1994, **98**, 11623–11627.
36 J. S. Binkley, J. A. Pople and W. J. Hehre, *J. Am. Chem. Soc.*, 1980, **102**, 939–947.
37 S. F. Boys and F. Bernardi, *Mol. Phys.*, 1970, **19**, 553–571.
38 B. Paizs, P. Salbador, A. G. Császár, M. Duran and S. Sohai, *J. Comput. Chem.*, 2001, **22**, 196–207.
39 R. F. W. Bader, *Atoms in Molecules. A Quantum Theory*, Clarendon, Oxford University Press, Oxford, 1990.
40 F. Biegler-König, J. Schönbohm and D. Bayles, *J. Comput. Chem.*, 2001, **22**, 545–559.
41 A. E. Reed, L. A. Curtiss and F. Weinhold, *Chem. Rev.*, 1988, **88**, 899–926.
42 R. Ditchfield, *Mol. Phys.*, 1974, **27**, 789–807.

43 K. Wolinski, J. F. Hilton and P. Pulay, *J. Am. Chem. Soc.*, 1990, **112**, 8251–8260.
44 M. J. Frisch, G. W. Trucks, H. B. Schlegel, G. E. Scuseria, M. A. Robb, J. R. Cheeseman, J. A. Montgomery, Jr., T. Vreven, K. N. Kudin, J. C. Burant, J. M. Millam, S. S. Iyengar, J. Tomasi, V. Barone, B. Mennucci, M. Cossi, G. Scalmani, N. Rega, G. A. Petersson, H. Nakatsuji, M. Hada, M. Ehara, K. Toyota, R. Fukuda, J. Hasegawa, M. Ishida, T. Nakajima, Y. Honda, O. Kitao, H. Nakai, M. Klene, X. Li, J. E. Knox, H. P. Hratchian, J. B. Cross, V. Bakken, C. Adamo, J. Jaramillo, R. Gomperts, R. E. Stratmann, O. Yazyev, A. J. Austin, R. Cammi, C. Pomelli, J. Ochterski, P. Y. Ayala, K. Morokuma, G. A. Voth, P. Salvador, J. J. Dannenberg, V. G. Zakrzewski, S. Dapprich, A. D. Daniels, M. C. Strain, O. Farkas, D. K. Malick, A. D. Rabuck, K. Raghavachari, J. B. Foresman, J. V. Ortiz, Q. Cui, A. G. Baboul, S. Clifford, J. Cioslowski, B. B. Stefanov, G. Liu, A. Liashenko, P. Piskorz, I. Komaromi, R. L. Martin, D. J. Fox, T. Keith, M. A. Al-Laham, C. Y. Peng, A. Nanayakkara, M. Challacombe, P. M. W. Gill, B. G. Johnson, W. Chen, M. W. Wong, C. Gonzalez and J. A. Pople, *GAUSSIAN 03 (Revision B.03)*, Gaussian, Inc., Wallingford, CT, 2004.
45 S. N. Thakur, S. K. Tiwari and D. K. Rai, *J. Mol. Struct.*, 1970, **5**, 309–319.
46 J. J. Stezowski, T. J. Brett, S. Liu and P. Coppens, *Chem. Commun.*, 1999, 551–552.
47 X. S. Liu, H. J. Chen and L. M. He, *Probability Theory & Mathematical Statistics*, Scientific press, Beijing, 3rd edn, 2002, pp. 293–304.
48 T. Nakanaga, F. Ito, J. Miyawadi, K. Sugawara and H. Takeo, *Chem. Phys. Lett.*, 1996, **261**, 414–420.
49 T. Nakanaga and F. Ito, *J. Mol. Struct.*, 2003, **649**, 105–110.
50 F. F. Gao, G. S. Zhu, Y. Chen, Y. Li and S. L. Qiu, *J. Phys. Chem. B*, 2004, **108**, 3426–3430.
51 U. Koch and P. L. A. Popelier, *J. Phys. Chem. A*, 1995, **99**, 9747–9754.
52 P. L. A. Popelier, *Atoms in Molecules. An Introduction*, Pearson Education, Harlow, 1999.
53 H. A. Carlson, J. M. Briggs and J. A. McCammon, *J. Med. Chem.*, 1999, **42**, 109–117.
54 G. W. Muth, L. Ortoleva-Donnelly and S. A. Strobel, *Science*, 2000, **289**, 947–950.
55 T. Jones and G. Taylor, *Proc.-Eur. Congr. Biopharm. Pharmacokinet.*, 1987, **2**, 181–190.
56 P. Huyskens and T. Zeegers-Huyskens, *J. Chim. Phys.*, 1964, **61**, 81–86.
57 A. Albert and E. P. Serjeant, *Ionization Constants of Acids and Based*, Methuen, London, 1962.
58 D. D. Perrin, *Dissociation Constants of Organic Bases in Aqueous Solution*, Butterworth, London, 1965.
59 J. E. D. Bene and M. J. T. Jordan, *J. Am. Chem. Soc.*, 2000, **122**, 4794–4797.
60 A. E. Shchavlev, A. N. Pankratov and V. Enchev, *J. Phys. Chem. A*, 2007, **111**, 7112–7123.
61 SDBSWeb: http://riodb01.ibase.aist.go.jp/sdbs/ (National Institute of Advanced Industrial Science and Technology, date of access).
62 T. Axenrod, P. S. Pregosin, M. J. Wieder, E. D. Becker, R. B. Bradley and G. W. A. Milne, *J. Am. Chem. Soc.*, 1971, **93**, 6536–6541.
63 R. J. Abraham, J. J. Byrne, L. Griffiths and M. Perez1, *Magn. Reson. Chem.*, 2006, **44**, 491–509.
64 I. C. Jones, G. J. Sharman and J. Pidgeon, *Magn. Reson. Chem.*, 2005, **43**, 497–509.
65 I. Ando, S. Kuroki, H. Kurosu and T. Yamanobe, *Prog. Nucl. Magn. Reson. Spectrosc.*, 2001, **39**, 79–133.
66 L. F. Pacios and P. C. Gómez, *J. Phys. Chem. A*, 2004, **108**, 11783–11792.

